PHYSICAL REVIEW A VOLUME 24, NUMBER 1 JULY 1981

Two-body rearrangement collision of atom–diatomic-molecule system: Role of wave-number matching

S. H. Suck and R. W. Emmons

Department of Physics and Graduate Center for Cloud Physics Research, University of Missouri at Rolla, Rolla, Missouri 65401

(Received 18 November 1980)

A concise interpretation of the perturbation potential in the distorted-wave Born-approximation representation is given for state-to-state rearrangement collisions. We discuss the usefulness of the kernel and radial overlap distributions for understanding reaction mechanisms. For example, the cause of backward scattering in product angular distributions is explained from the study of the kernel distribution. The reaction zone is seen to be well defined by the domain of the kernel distribution with the exclusion of the region interior to the channel radii corresponding to the classical turning points in the initial- and final-arrangement channels. However, the domain of the overlap distribution sharply defines the reaction zone on the channel coordinate plane. Unlike the case of a few nucleon transfer reaction involving a massive target nucleus, wave-number matching alone is not a sufficient condition for yielding the maximum cross sections for the state-to-state rearrangement-collision processes of heterotriatomic systems.

I. INTRODUCTION

One of the frequently used quantum-mechanical methods for the study of rearrangement collisions (reactive scattering) is the DWBA (distorted-wave Born-approximation).[1-14] The DWBA is best served for one-step collision processes which occur as a consequence of negligible coupling between the entrance channel and inelastic channels in the initial-arrangement channel, and between the exit channel and inelastic channels in the final-arrangement channel. In such direct reactions, particles (wave packets) in each arrangement are propagated with negligible time delay. Thus, in the DWBA theory for rearrangement collisions, the transition is assumed to occur between elastic-scattering states which belong to the two different arrangement channels.

In our present DWBA[13] study, we do not attempt to report excessive computed results of product angular distributions. Instead, we focus our attention on physical factors which determine the structures of angular distributions for the less understood reactive scattering of atom–diatomic-molecular systems. The collision-energy-independent kernel (Eq. 34) describes the internal properties of the state-to-state reactive system.[14] The radial overlap integral (Eq. 33) defines the overlap "strength" between the energy-independent ("internal") part, namely, the kernel, and the energy-dependent ("external") parts, namely, the initial and final partial (distorted) waves. Thus, it is of great interest to investigate separately the internal and external contributions to the structure of the product angular distributions. For this reason we will pay attention to the distributions of both the kernel and radial overlap on the channel-radii (coordinates) plane defined by the initial- and final-channel coordinates. In addition, we present a concise interpretation of the perturbation interaction which appears in the DWBA formalism.[13]

To quickly acquaint the readers with the present work, we briefly list the general contents. In Sec. II, the perturbation potential of the DWBA for rearrangement collisions is interpreted in terms of the projection operator. The kernel and radial overlap integral, which contain the perturbation potential, are defined for the atom–diatomic-molecule system in Sec. III. In addition, all the triangular inequalities necessary for the complete description of the DWBA are listed. In Sec. IV, we analyze the radial overlap integral with particular emphasis on wave-number matching. After a brief description of extracting the distorting potential for the present DWBA calculations, we discuss the computed results of the kernel, radial overlap integral, angular distributions, and excitation functions in Sec. V. In the final Sec. VI, discussions regarding future improvements over the present DWBA will be presented along with a summary of this work.

II. INTERPRETATION OF PERTURBATION INTERACTION CAUSING REACTIVE SCATTERING

Consider two-body interactions leading to two-body breakup reactions,

$$x+X=(y+a)+X \leftrightarrows (a+X)+y=Y+y\,. \tag{1}$$

Here, x and X are the incoming projectile and target, respectively; y and Y are the outgoing projectile and residual particles. The forward direction is the stripping process and the reverse direction, the pickup process. Such terminology refers to the event that occurs to the projectile. All or part of the particles above can be composite systems.

The Hamiltonian for the two-body collisions is conveniently partitioned for the initial α and final β arrangement channels,

$$H=H_\alpha=H_\beta\,, \tag{2}$$

where

$$H_\alpha=h_\alpha+H'_\alpha\,, \tag{3a}$$

and

$$H_\beta=h_\beta+H'_\beta\,, \tag{3b}$$

assuming that the internal motion is uncoupled to the external motion. Here, $h_\alpha(h_\beta)$ describes the internal motions of the composite systems, both incoming (outgoing) projectile and target (residual) particles. The relative (external) motion in the initial-(final-)arrangement channel is described by $H'_\alpha(H'_\beta)$,

$$H'_\alpha=T_\alpha+U_\alpha\,, \tag{4a}$$

and

$$H'_\beta=T_\beta+U_\beta\,, \tag{4b}$$

where $T_\alpha(T_\beta)$ is the relative kinetic energy and $U_\alpha(U_\beta)$, the interaction-energy part of the Hamiltonian. The interaction $U_\alpha(U_\beta)$ between the colliding (departing) pairs can be further subdivided,

$$U_\alpha=PU_\alpha P+(1-P)U_\alpha P+PU_\alpha(1-P)+(1-P)U_\alpha(1-P)\,, \tag{5}$$

with P being the projection operator, $P^2=P$. The projection operator P is defined to project onto a state of the entrance channel. Under this definition, the first term $PU_\alpha P$ obviously corresponds to the distorting potential which opens only a single channel, thus describing elastic-scattering waves (uncoupled distorted waves). For the DWBA representation, the complementary projection operator $(1-P)$ is defined to project onto a state of the final-arrangement channel.

The two potential Hamiltonians for the description of the DWBA are

$$H_\alpha=H^0_\alpha+PU_\alpha P+W_\alpha \tag{6a}$$

and

$$H_\beta=H^0_\beta+PU_\beta P+W_\beta\,, \tag{6b}$$

where

$$H^0_\alpha=h_\alpha+T_\alpha\,, \tag{7a}$$

$$H^0_\beta=h_\beta+T_\beta\,, \tag{7b}$$

$$W_\alpha=U_\alpha-PU_\alpha P\,, \tag{8}$$

and

$$W_\beta=U_\beta-PU_\beta P\,. \tag{9}$$

In what follows, we choose the prior form of the interaction potential.

The integral equation that satisfies the boundary condition of an outgoing wave is

$$\Psi^{(+)}_\alpha=X^{(+)}_\alpha+g^+_\alpha\;W_\alpha X^{(+)}_\alpha\,, \tag{10}$$

or

$$\Psi^{(+)}_\alpha=X^{(+)}_\alpha+g^+_\alpha(U_\alpha-PU_\alpha P)X^{(+)}_\alpha\;, \tag{11}$$

with the Green's function

$$g^+_\alpha=g^+_{1\alpha}+g^+_{1\alpha}W_\alpha g^+\,, \tag{12}$$

where

$$g^+_{1\alpha}=[E-(H^0_\alpha+PU_\alpha P)+i\epsilon]^{-1}\,. \tag{13}$$

Now for $X^{(+)}_\alpha$, we write

$$X^{(+)}_\alpha=\Phi_\alpha+g^+_{1\alpha}(PU_\alpha P)\Phi_\alpha\,. \tag{14}$$

Φ_α is the plane-wave solution.

The Gell-Mann Goldberger transformation[1] leads to the T-matrix element,

$$T_{\beta\alpha}=\langle\Phi_\beta|PU_\alpha P|X^{(+)}_\alpha\rangle+\langle X^{(-)}_\beta|U_\alpha-PU_\alpha P|\Psi^{(+)}_\alpha\rangle\,. \tag{15}$$

The substitution of (11) and (14) into (15) yields

$$T_{\beta\alpha}=\langle\Phi_\beta|PU_\alpha P+PU_\alpha Pg^+_{1\alpha}PU_\alpha P|\Phi_\alpha\rangle+\langle X^{(-)}_\beta|U_\alpha-PU_\alpha P+(U_\alpha-PU_\alpha P)g^+_\alpha(U_\alpha-PU_\alpha P)|X^{(+)}_\alpha\rangle\,. \tag{16}$$

The first Born approximation yields

$$T_{\beta\alpha}=\langle\Phi_\beta|PU_\alpha P|\Phi_\alpha\rangle+\langle X^{(-)}_\beta|U_\alpha-PU_\alpha P|X^{(+)}_\alpha\rangle\,. \tag{17}$$

In the case of negligible contribution by the first term above, we simply have the commonly expressed DWBA transition amplitude of the form

$$T^{\mathrm{DWBA}}_{\beta\alpha}=\langle X^{(-)}_\beta|U_\alpha-PU_\alpha P|X^{(+)}_\alpha\rangle\,, \tag{18}$$

or from (8),

$$T^{\mathrm{DWBA}}_{\beta\alpha}=\langle X^{(-)}_\beta|W_\alpha|X^{(+)}_\alpha\rangle\,. \tag{19}$$

The use of (5) and

$$(1-P)|X^{(+)}_\alpha\rangle=0 \tag{20}$$

reduces the T-matrix element to

$$T^{\mathrm{DWBA}}_{\beta\alpha}=\langle X^{(-)}_\beta|(1-P)U_\alpha P|X^{(+)}_\alpha\rangle\,. \tag{21}$$

From (19) and (21), it is clear that the W_α defined in (8) is now the perturbation interaction which can be regarded as the cause of the reactive transition from a state of the entrance channel α to a state of the final-arrangement channel β. In the DWBA representation of the rearrangement collision, the operator $(1-P)$ is then the projection operator which projects onto a state in the new arrangement channel. Finally, we write (18) more explicitly by noting that $X_\alpha=\chi_\alpha\phi_x\phi_X$ and $X_\beta=\chi_\beta\phi_y\phi_Y$ due to (3),

$$T_{\beta\alpha}^{\mathrm{DWBA}} = \int \chi_\beta^{(-)*} \langle \phi_y \phi_Y | W_\alpha | \phi_x \phi_X \rangle \chi_\alpha^{(+)} d\vec{R}_a d\vec{R}_b . \tag{22}$$

Here ϕ_i is the internal wave function of the particle i ($i = x, X, y, Y$) and $\chi_\alpha(\chi_\beta)$ is the distorted-wave function which describes the relative motion of the two particles in the initial (final) channel. $\vec{R}_a(\vec{R}_b)$ is the initial- (final-) channel coordinate vector.

III. KERNEL AND RADIAL OVERLAP ON THE CHANNEL RADII PLANE (R_a, R_b)

In what follows below, we bring attention only to essentials, as details are found in the literature.[13] We consider the two-body rearrangement collision of the atom–diatomic-molecule system, $A + BC \to AB + C$, where $A = x$, $BC = X$, $AB = Y$, and $C = y$. The rearrangement transition from the vibrational (n_a) and rotational (j_a, m_a) state of the reactant molecule BC to the vibrational (n_b) and rotational (j_b, m_b) state of the product molecule AB is described by

$$T_{n_b j_b m_b ; n_a j_a m_a}^{\mathrm{DWBA}} = J \int \chi_\beta^{(-)*}(\vec{K}_b, \vec{R}_b) \phi_{n_b j_b m_b}^{*}(\vec{r}_b) W_\alpha(\vec{R}_a, \vec{r}_a) \times \phi_{n_a j_a m_a}(\vec{r}_a) \chi_\alpha^{(+)}(\vec{K}_a, \vec{R}_a) d\vec{R}_a d\vec{R}_b . \tag{23}$$

J is the Jacobian of the transformation from the internal coordinates (interatomic displacements of the diatomic molecules) $\vec{r}_a$ and $\vec{r}_b$ to the external (channel or relative) coordinates $\vec{R}_a$ and $\vec{R}_b$. $\vec{K}_a(\vec{K}_b)$ is the wave vector for the relative motion in the initial- (final-) arrangement channel.

We introduce the transferred angular momentum j during reaction

$$\vec{j} = \vec{j}_b - \vec{j}_a = \vec{L}_a - \vec{L}_b \tag{24}$$

as a consequence of the conservation of the total angular momentum $\vec{J}$,

$$\vec{J} = \vec{j}_a + \vec{L}_a = \vec{j}_b + \vec{L}_b , \tag{25}$$

in which $\vec{L}_a(\vec{L}_b)$ is the orbital angular momentum of the initial-(final-) arrangement channel. It immediately follows that

$$T_{n_b j_b m_b ; n_a j_a m_a}^{\mathrm{DWBA}} = J \sum_{jm} (-1)^{m_a} \langle j_b j_a m_b - m_a | jm \rangle \times \int \chi_\beta^{(-)*}(\vec{K}_b, \vec{R}_b) \vec{W}_\alpha(\vec{R}_a, \vec{r}_a) \chi_\alpha^{(+)}(\vec{K}_a, \vec{R}_a) [\phi_{j_b m_b}^{*}(\vec{r}_b) \phi_{j_a m_a}(\vec{r}_a)]_{jm} d\vec{R}_b d\vec{R}_a , \tag{26}$$

where

$$[\phi_{j_b m_b}^{*}(\vec{r}_b) \phi_{j_a m_a}(\vec{r}_a)]_{jm} = \sum_{m_b} (-1)^{m_a} \langle j_b j_a m_b - m_a | jm \rangle \phi_{j_b m_b}^{*}(\vec{r}_b) \phi_{j_a m_a}(\vec{r}_a) . \tag{27}$$

The summation of the squared value of the transition amplitude over the z components m_a and m_b leads to the incoherent sum over the transferred angular momentum,

$$\sum_{m_a m_b} | T_{n_b j_b m_b ; n_a j_a m_a} |^2 = \sum_{jm} | t_{jm}(\theta) |^2 , \tag{28}$$

with

$$t_{jm}(\theta) = i^{j - j_a - j_b} (-1)^{(|m| - m)/2} (2\pi / K_b K_a) J (2j_a + 1)(2j_b + 1) \times \sum_{L_a L_b} i^{-L_a - L_b} e^{i(\sigma_{L_a} + \sigma_{L_b})} [(2L_a + 1)(2L_b + 1)]^{1/2} \left(\frac{(L_b - |m|)!}{(L_b + |m|)!} \right)^{1/2} P_{L_b}^{|m|}(\theta) \langle L_b L_a m o | jm \rangle \times \sum_{k \lambda_a \lambda_b} (-1)^{\lambda_b - \lambda_a} (2k + 1) \binom{2j_a}{2\lambda_a}^{1/2} \binom{2j_b}{2\lambda_b}^{1/2} Z_{L_b L_a j}^{j_b j_a \lambda_b \lambda_a k} S_{L_b L_a}^{j_b j_a \lambda_b \lambda_a k} . \tag{29}$$

Here, σ_{L_i} is the phase shift in rearrangement channel i and $\binom{m}{n}$ is the binomial coefficient. The angular momentum factor Z is given by

$$Z_{L_b L_a j}^{j_b j_a \lambda_b \lambda_a k} = \sum_{d_a d_b} \langle d_b k 0 0 | L_b 0 \rangle \langle d_a k 0 0 | L_a 0 \rangle W(d_b L_b d_a L_a ; kj) [(2d_a + 1)(2d_b + 1)]^{1/2} \langle j_b - \lambda_b \lambda_a 0 0 | d_b 0 \rangle \langle j_a - \lambda_a \lambda_b 0 0 | d_a 0 \rangle \begin{bmatrix} \lambda_b & j_a - \lambda_a & d_a \\ j_b - \lambda_b & \lambda_a & d_b \\ j_b & j_a & j \end{bmatrix} , \tag{30}$$

$W(a, b, c, d; ef)$ and $\begin{bmatrix} j_1 & j_2 & J_{12} \\ j_3 & j_4 & J_{34} \\ J_{13} & J_{14} & J \end{bmatrix}$

are, respectively, the Racah coefficient and $9-j$ symbol. The summing indices (λ_a, λ_b, d_a, d_b and k) came into existence as a result of angular integration processes. Listed below are all the necessary triangular inequalities to be satisfied for the sums that appear in the DWBA expression,

$$|j_a-j_b| \leqslant j \leqslant j_a+j_b\,, \tag{31a}$$

$$|L_a-j| \leqslant L_b \leqslant L_a+j\,, \tag{31b}$$

$$0 \leqslant \lambda_a \leqslant j_a\,, \tag{31c}$$

$$0 \leqslant \lambda_b \leqslant j_b\,, \tag{31d}$$

$$|j_a-\lambda_a-\lambda_b| \leqslant d_a \leqslant j_a-\lambda_a+\lambda_b\,, \tag{31e}$$

$$|j_b-\lambda_b-\lambda_a| \leqslant d_b \leqslant j-\lambda_b+\lambda_a\,, \tag{31f}$$

$$|d_a-j| \leqslant d_b \leqslant d_a+j\,, \tag{31g}$$

$$|L_a-d_a| \leqslant k \leqslant L_a+d_a\,, \tag{31h}$$

and

$$|L_b-d_b| \leqslant k \leqslant L_b+d_b\,. \tag{31i}$$

The overlap integral factor S above is defined by

$$S_{L_bL_a}^{j_bj_a\lambda_b\lambda_ak} = s_b^{\lambda_b} t_b^{j_b-\lambda_b} s_a^{j_a-\lambda_a} t_a^{\lambda_a} I_{L_bL_a}^{j_bj_a\lambda_b\lambda_ak}\,, \tag{32}$$

with the mass factors (s_a, t_a, s_b, and t_b) defined in the literature.[13] Here, the radial overlap integral I is given by

$$I_{L_bL_a}^{j_bj_a\lambda_b\lambda_ak} = \int \chi_{L_b}(K_b,R_b) G_k^{j_bj_a}(R_b,R_a) \chi_{L_a}(K_a,R_a) \times R_b^{j_b-\lambda_b+\lambda_a+1} R_a^{j_a-\lambda_a+\lambda_b+1} dR_a dR_b\,, \tag{33}$$

in which the kernel G is simply

$$G_k^{j_bj_a}(R_b,R_a) = \int_{-1}^{1} [u_{j_b}(r_b)/r_b^{j_b}] W(\vec{\mathrm{R}}_a,\vec{\mathrm{r}}_a) \times [u_{j_a}(r_a)/r_a^{j_a}] P_k(\mu) d\mu\,, \tag{34}$$

with

$$\mu = \vec{\mathrm{R}}_a \cdot \vec{\mathrm{R}}_b/(R_aR_b)\,. \tag{35}$$

Here, $u_{j_a}(r_a)/r_a$ ($u_{j_b}(r_b)/r_b$) is the radial part of the wave function of the reactant (product) molecule. As can be seen here, the kernel is the energy-independent part of the contribution, while the radial overlap integral contains both the energy-dependent and energy-independent contributions to the cross sections. The details of the kernel and radial overlap will be explored later.

IV. WAVE-NUMBER MATCHING CONDITION FOR COLLINEAR REACTION

It is now obvious from (33) that a good overlap is necessary for yielding large cross sections. Such a situation will occur if the partial waves (χ_{L_a} and χ_{L_b}) overlap well with the dominant region of the kernel distribution. As an example, we consider here the case of collinearly favored reactions.

The linear relationship between the channel coordinates and internal coordinates is

$$\begin{pmatrix} R_a \\ R_b \end{pmatrix} = \begin{pmatrix} \dfrac{M_C}{M_B+M_C} & 1 \\ 1 & \dfrac{M_A}{M_A+M_B} \end{pmatrix} \begin{pmatrix} r_a \\ r_b \end{pmatrix} \tag{36}$$

for the collinear configuration of the triatomic system ABC. M_i is the mass of the atom i ($i=A$, B, and C). We find, by using the internal coordinate r_a of the reactant molecule BC,

$$R_b = mR_a + b\,, \tag{37a}$$

where

$$m = M_A/(M_A+M_B)\,, \tag{37b}$$

and

$$b = b_0 r_a\,, \tag{37c}$$

with

$$b_0 = M_B(M_A+M_B+M_C)/[(M_A+M_B)(M_B+M_C)]\,, \tag{37d}$$

or by using the internal coordinate r_b of the product molecule AB,

$$R_b = nR_a + c\,, \tag{38a}$$

where

$$n = (M_B+M_C)/M_C\,, \tag{38b}$$

and

$$c = c_0 r_b\,, \tag{38c}$$

with

$$c_0 = -M_B(M_A+M_B+M_C)/[M_C(M_A+M_B)]\,. \tag{38d}$$

The kernel distribution for the collinearly favored reactions can be approximated as

$$G_R(R_b,R_a) \simeq G_k^0(R_b)\delta(R_b-mR_a-b)\,. \tag{39}$$

Here, $G_k^0(R_b)$ is the value of the kernel at $R_b=mR_a+b$.

Later it will be seen that the kernel distribution for the collinear raction located near the lines with the slopes m and n, and with their intercepts b and c in which r_a^0 and r_b^0 are taken as equilibrium distances of the diatomic molecules AB and BC, respectively.

The substitution of (39) into (33) yields

$$I_{L_bL_a}^{j_bj_a\lambda_b\lambda_ak} \simeq \int \chi_{L_b}(K_b, mR_a+b) G_k^0(mR_a+b) \chi_{L_a}(K_a,R_a) \times (mR_a+b)^{j_b-\lambda_b+\lambda_a+1} R_a^{j_a-\lambda_a+\lambda_b+1} dR_a\,, \tag{40}$$

where the range of k is

$$\min(L_a, L_b) \leqslant k \leqslant \max(L_a+j_a+j_b, L_b+j_a+j_b)\,, \tag{41}$$

as can be verified from (31).

For the particular case of rotational ground-state transitions, $k=L_a=L_b$. The best overlap occurs with the following conditions: (1) wave number matching $K_a \simeq K_b$, (2) occurrence of the classical turning points at nearly same channel coordinates $R_a^0 \simeq R_b^0$, and (3) mass ratios with $m \simeq 1$ and $b_0/m \ll 1$.

In general, the state-to-state reactive (rearrangement collision) scattering process is likely to prefer nonzero transferred angular momenta unless $|K_b R_b^0 - K_a R_a^0| = 0$. Unlike the case of a few nucleon transfer reaction involving a massive target nucleus,[2] wave-number matching is not generally sufficient to yield the maximum contribution to cross sections for heterotriatomic systems. For identical triatomic systems, the condition of wave-number matching alone may, in general, be sufficient. For the heterotriatomic systems, the two classical turning points are not likely to easily occur at the same distances. Thus, angular momentum mismatch is favored even in the reaction which involves wave-number matching. If the lower (smaller orbital angular momentum) partial waves yield better overlap compared to the higher ones, the product angular distributions will favor backward scattering for the collinear atom-diatom reactive system.

From the conservation of the total energy, we write

$$E = T_\alpha + \epsilon_\alpha \mp \Delta E^0 = T_\beta + \epsilon_\beta\ . \tag{42}$$

$\epsilon_\alpha(\epsilon_\beta)$ is the internal (rovibrational) energy in the initial (final) channel. The zero of the internal energy is defined at the zero-point vibrational energy. ΔE^0 is the difference between the potential-energy depths V_α^0 and V_β^0 where the zero-point vibrational energies of the reactant and product diatomic molecules occur:

$$\Delta E^0 = V_\beta^0 - V_\alpha^0\,, \tag{43}$$

Thus, the zero of the total energy is the larger (in absolute magnitude) of the two potential depths V_α^0 and V_β^0. The negative (positive) sign is for exoergicity (endoergicity).

Now we write

$$K_a = \{2\mu_\alpha[T_\alpha - U_{00}^\alpha(R_a)]\}^{1/2} \tag{44}$$

and

$$K_b = \{2\mu_\beta[T_\beta - U_{00}^\beta(R_b)]\}^{1/2}\,. \tag{45}$$

Here, $U_{00}^\alpha(U_{00}^\beta)$ is the initial (final) channel distorting potential. Using (42), we find the linear relationship for wave-number matching $K_a = K_b$,

$$\begin{pmatrix} T_\alpha \\ T_\beta \end{pmatrix} = \frac{1}{\mu_\beta - \mu_\alpha} \begin{pmatrix} \mu_\beta & 1 \\ \mu_\alpha & 1 \end{pmatrix} \begin{pmatrix} \Delta\epsilon_\pm \\ \Delta U \end{pmatrix}, \tag{46}$$

in which

$$\Delta\epsilon_+ = \epsilon_\beta - \epsilon_\alpha + \Delta E^0\,, \tag{47a}$$

for exoergicity;

$$\Delta\epsilon_- = \epsilon_\beta - \epsilon_\alpha - \Delta E^0\,, \tag{47b}$$

for endoergicity,

and

$$\Delta U = \mu_\beta U_{00}^\beta - \mu_\alpha U_{00}^\alpha\,. \tag{48}$$

Here, $\mu_\alpha(\mu_\beta)$ is the reduced mass in the initial (final) arrangement, i.e.,

$$\mu_\alpha = M_A(M_B+M_C)/(M_A+M_B+M_C)\,, \tag{49a}$$

and

$$\mu_\beta = M_C(M_A+M_B)/(M_A+M_B+M_C)\,, \tag{49b}$$

for $A+BC \to AB+C$.

$\Delta\epsilon_+(\Delta\epsilon_-)$ measures the rovibrational energy difference between the two diatomic molecules with the reference energy level at the zero-point vibrational energy of the reactant (product) molecule. ΔU is simply the mass-weighted distorting potential difference between the final and initial channels. Note that the relation (46) satisfies any reaction, both collinear and noncollinear.

V. DISCUSSIONS OF DISTORTING POTENTIAL AND COMPUTED DWBA RESULTS

For the distorting potential PUP needed for the solution of the distorted-wave function, one can use the diagonal term that appears in the coupled Schrödinger equation. Otherwise, the optical model potential which fits elastic-scattering data is well suited for the description of the distorted-wave functions as commonly used in the study of nuclear reactions. However, the phenomenological optical potential is not readily available for the two-body interaction problem of the atom–diatomic-molecule system. In what follows below, we first present a brief discussion on the extraction of the distorting potentials consistent with the Hamiltonian (3) defined earlier.

In accordance with the Hamiltonian, the complete function is written:

$$\Psi^{JM}_{n_a j_a L_a}(\vec{\mathrm{R}}_i, \vec{\mathrm{r}}_i) = \sum_{\substack{n'_a j'_a L'_a \\ m'_a M'_a \\ k}} [\chi^J_{n'_a j'_a L'_a;\, n_a j_a L_a}(R_k)/R_k][u_{n'_a j'_a}(r_k)/r_k]\langle j'_a L'_a m'_a M'_a | JM\rangle Y_{L'_a M'_a}(\hat{R}_k) Y_{j'_a m'_a}(\hat{r}_k)\,. \tag{50}$$

Here, k runs over all the arrangements, $k=\alpha$, β, and γ for the triatomic system. i is to denote the initial arrangement. Now the scalar product of the Schrödinger equation,

$$H\Psi^{JM}_{n_a j_a L_a}(\vec{\mathrm{R}}_i,\vec{\mathrm{r}}_i)=E\Psi^{JM}_{n_a j_a L_a}(\vec{\mathrm{R}}_i,\vec{\mathrm{r}}_i) \tag{51}$$

by the product of the radial wave function $u_{n_a' j_a'}(r_\alpha)/r_\alpha$

and

$$y^{JM}_{j_a' L_a'}(\hat{R}_\alpha,\hat{r}_\alpha)=\sum\langle j_a' L_a' m_a' M_a' \,|JM\rangle Y_{L_a' M_a'}(\hat{R}_\alpha)Y_{j_a' m_a'}(\hat{r}_\alpha) \tag{52}$$

yields the set of the coupled differential equations,

$$\begin{aligned}
&\frac{-\hbar^2}{2\mu_\alpha}\left(\frac{d^2}{dR_\alpha^2}-\frac{L_a'(L_a'+1)}{R_\alpha^2}+K^2_{n_a' j_a'}\right)\chi^J_{n_a' j_a' L_a';n_a j_a L_a}(R_\alpha)\\
&\quad=-\sum_{n_a'' j_a'' L_a''}\langle n_a' j_a' L_a' |\,V\,| n_a'' j_a'' L_a''\rangle^J \chi^J_{n_a'' j_a'' L_a'';n_a j_a L_a}(R_\alpha)\\
&\quad\quad-\sum_{\substack{n_b j_b L_b\\ k\neq\alpha}}\int d^3r\, d^2\hat{R}_\alpha\, u_{n_a' j_a'}/r_\alpha\, y^{JM}_{j_a' L_a'}(\hat{R}_\alpha,\hat{r}_\alpha)(H-E)u_{n_b j_b}(r_k)/r_k\, y^{JM}_{j_b L_b}(\hat{R}_k,\hat{r}_k)\chi^J_{n_b j_b L_b;n_a j_a L_a}(R_k)\,.
\end{aligned} \tag{53}$$

The first term on the right describes coupling with the inelastic channels in the arrangement channel α. Coupling with the states of other arrangement channels appears in the second term. V is the two-body interaction potential in the arrangement channel α.

For application to the DWBA, we focus our attention on the potential matrix element given by[15,16]

$$\begin{aligned}
\langle n_a' j_a' L_a' |\,V\,| n_a j_a L_a\rangle^J &=(-1)^{j_a+j_a'+J}[(2j_a+1)(2j_a'+1)(2L_a+1)(2L_a'+1)]^{1/2}\\
&\quad\times\sum_j U^j_{n_a' j_a';n_a j_a}(R_a)\langle j_a j_a' 00\,|j0\rangle\langle L_a L_a' 00\,|j0\rangle\, W(j_a L_a j_a' L_a';Jj)\,/\sqrt{2j+1}\,,
\end{aligned} \tag{54}$$

where

$$\begin{aligned}
&U^j_{n_a' j_a';n_a j_a}(R_a)\\
&\quad=\int dr_a u^*_{n_a' j_a'}(r_a)V^j_\alpha(R_a,r_a)u_{n_a j_a}(r_a)\,.
\end{aligned} \tag{55}$$

Here the subscript α for the arrangement of $A+BC$ is simply replaced by a. It is obvious that the diagonal term corresponds to the first term PUP in (5). This is then the distorting potential to be used for the description of the DWBA transition amplitude. For the rotational ground-state reactive transitions, the distorting potentials become

$$U^\alpha_{00}=\int dr_a\, U^*_{n_a 0}(r_a)V^{j=0}_\alpha(R_a,r_a)U_{n_a 0}(r_a) \tag{56a}$$

for the initial-arrangement channel α, and

$$U^\beta_{00}=\int dr_b U^*_{n_b 0}(r_b)V^{j=0}_\beta(R_b,r_b)U_{n_b 0}(r_b) \tag{56b}$$

for the final-arrangement channel.

For completeness, we formally discuss the optical model potential that is suited for the DWBA. From the elimination of all channels except the entrance channel, the coupled equations in matrix form are

$$(T+\tilde{U}_{00}-E)\chi_0=-\tilde{U}_{0I}\chi_I \tag{57}$$

and

$$(T+\tilde{U}_{II}-E)\chi_I=-\tilde{U}_{I0}\chi_0\,. \tag{58}$$

Here, 0 is to denote the entrance channel and I, the rest of the channels. Thus, the column vector χ_I is given by

$$\chi_I=\begin{bmatrix}\chi_1\\ \chi_2\\ \cdot\\ \cdot\\ \cdot\end{bmatrix}. \tag{59}$$

$\tilde{U}$ is the potential-energy matrix and E is the energy matrix,

$$E=\frac{-\hbar^2 K_i^2}{2\mu_i}\delta_{ij}\,. \tag{60}$$

The introduction of (58) into (57) defines the optical model distorting potential U through

$$(T+U_{00}-E)\chi_0=0\,. \tag{61}$$

Here,

$$U_{00}=\tilde{U}_{00}-\tilde{U}_{0I}\frac{1}{T+\tilde{U}_{II}-E-i\epsilon}\tilde{U}_{I0}\,. \tag{62}$$

Finally, the prior form of the perturbation potential is, in general,

$$W_\alpha=U_\alpha-U_{00}^{\alpha}\,. \tag{63}$$

This is the form we have used in our present DWBA analysis.

For the DWBA study of angular distributions, we illustrate

$$\mathrm{F}+\mathrm{H}_2(n_a=0,\ j_a=0)\rightarrow \mathrm{HF}(n_b,j_b=0)+\mathrm{H}\,, \tag{64}$$

with $n_b=2$ or 3. The semiempirical Muckerman V LEPS potential surface[17,18] was employed to obtain the rotationally averaged distorting potential. For U_α in (63), we use

$$U_\alpha=V_{\mathrm{FHH}}-V_{\mathrm{HH}}\,, \tag{65}$$

where V_{FHH} is the LEPS potential surface and V_{HH}, the interatomic potential of the hydrogen molecule.

The magnitudes of cross sections are dependent on the degree of overlap between the kernel and partial waves as discussed earlier. In Fig. 1 the kernel distribution for the $(n_a=0,\ j_a=0)$ state to $(n_b=2,\ j_b=0)$ state is displayed on the channel-radii (coordinates) plane. A distinctive feature of this reaction is that the $|G_k|$ distribution is located near the two lines with the slopes $m\simeq 1$ and $n=2$ and their intercepts evaluated at the equilibrium interatomic distances of the reactant and product molecules, respectively. This indicates that preferential configuration during reaction is the collinear triatomic arrangement. The contour values are meaningful only in the order-of-magnitude sense (see the figure caption for more details). If the intermolecular interaction between the product molecule and projectile atom is repulsive, such collinearity will cause backward scattering in the product angular distribution. Unless the incident kinetic energy is exceedingly high, such backward scattering will tend to persist. We expect some notable shifts in angular distributions toward smaller c.m. (center-of-mass) scattering angles as the energy increases. The correctness of such conjecture will be found later. However, at considerably high energies, the DWBA may cease to be reliable as coupling with inelastic channels becomes increasingly significant. At still higher energies, a complete three-body breakup reaction leading to continuum will be a likelihood.

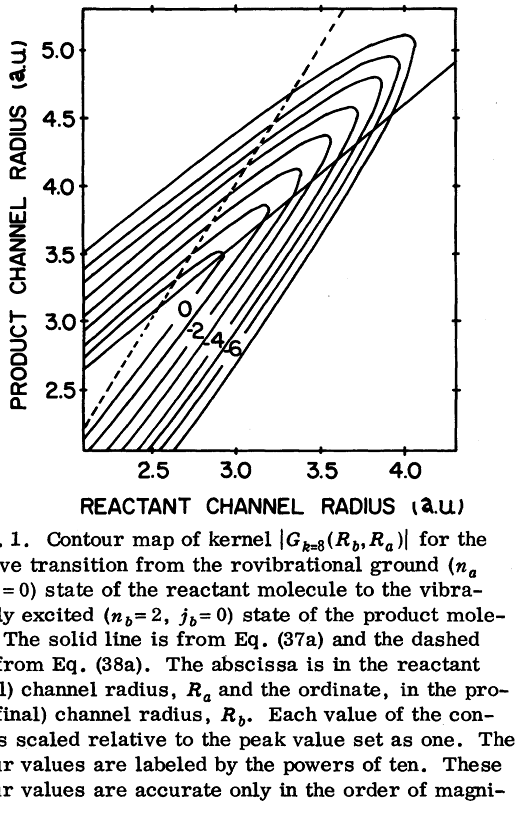

FIG. 1. Contour map of kernel $|G_{k=8}(R_b,R_a)|$ for the reactive transition from the rovibrational ground $(n_a=0,\ j_a=0)$ state of the reactant molecule to the vibrationally excited $(n_b=2,\ j_b=0)$ state of the product molecule. The solid line is from Eq. (37a) and the dashed line, from Eq. (38a). The abscissa is in the reactant (initial) channel radius, R_a and the ordinate, in the product (final) channel radius, R_b. Each value of the contour is scaled relative to the peak value set as one. The contour values are labeled by the powers of ten. These contour values are accurate only in the order of magnitude.

The kernel map shows that a large contribution comes from the region interior to the classical turning points. However, the reaction region will be substantially reduced due to the difficulty of "penetration" beyond the turning points. Indeed, this point is well understood from the radial overlap distribution $|\chi G\chi|$ shown in Fig. 2. The overlap region will increase with collision energy. This will, in turn, increase the reaction domain, thereby yielding larger cross sections. However, continuous increase of cross sections will not occur as will be seen later. At lower incident energies, the radial overlap between the kernel and distorted waves will be poorer. Only the smaller orbital angular momenta (impact parameters) will be good "participants" as they yield better overlap with the kernel than the larger ones do. Obviously, this causes more pronounced backward scattering. The angular distributions which display such features are plotted in Fig. 3 for the case of three different incident energies at 0.1 V, 0.2, V and 0.3 eV for the transition from $n_a=0$, $j_a=0$ to $n_b=2$, $j_b=0$. Note also that the radial overlap distribution did not significantly change the slope in the channel-coordinates plane.

Using (46) through (48), we obtain the best wave-number matching at the kinetic energy,

$$T_\alpha=\frac{\mu_\beta}{\mu_\beta-\mu_\alpha}(\epsilon_b-\epsilon_a+\Delta\epsilon)+\frac{1}{\mu_\beta-\mu_\alpha}(\mu_\beta U_{00}^{\beta}-\mu_\alpha U_{00}^{\alpha}) \tag{66}$$

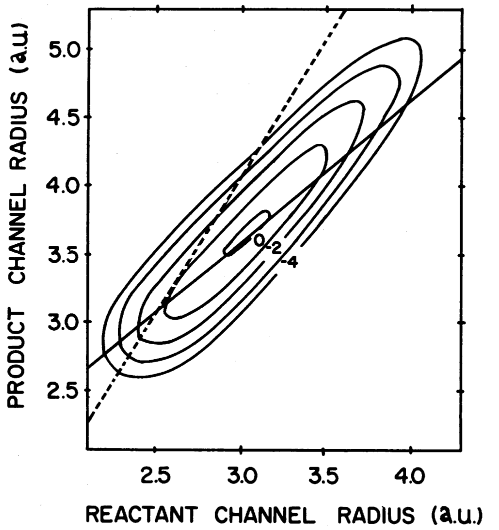

FIG. 2. Contour map of overlap distribution $|X_{L_b}G_kX_{L_a}|$ for the same transition (as in Fig. 1) with $L_b=L_a=k=8$ at the incident kinetic energy of 0.1 eV. The contour values are labeled in the same manner as in Fig. 1.

for exoergicity. The $F+H_2$ reactive scattering system is exoergic. For the above rovibrational transition, we find that with the Muckerman potential surface[17,18], the best wave-number matching occurs at the incident energy, $T_\alpha \simeq 0.45$ eV. At this energy, the classical turning point in the initial and final channels is found to satisfy $R_a^0 \approx R_b^0$ with $R_a \simeq 2.6$ a.u.. We find at these values, $\Delta U/\Delta\epsilon_+ \ll 1$. For the mass factors in (38) and (39), $m \simeq 1$ and $b_0/m \approx 0.5$. The last mass factor 0.5 does not exactly agree with the condition $b_0/m \ll 1$. However, it is interesting to note that the state-to-state cross section peaked near the incident energy of 0.45 eV, gradually declining thereafter. This is the energy where good wave-number matching was found. The excitation functions for the state-to-state rearrangement collision shown in Fig. 4 exemplifies this feature fairly well. For the reactive transition from the rovibrational ground state of the reactant molecule to the state $n_b=3$, $j_b=0$ of the product molecule, similar analysis was not feasible as several conditions were not satisfactorily met. However, the maximum position of the total cross section is expected to shift toward a lower energy as shown in the figure.

As is seen in Fig. 3, backward scattering (peak value of the differential cross section at the c.m. scattering angle of 180°) was predicted at the incident kinetic energy of 0.1 eV. Although not shown in the figure, such backward scattering features are more pronounced at lower incident energies. At incident kinetic energies about 0.2 eV, we find that sideways scattering (peak value of the differential cross section at the c.m. scattering angle less than 180°) occurred. Recently Lee *et al.*[19] have observed sideways scattering in their molecular beam measurements of $F+H_2$ ($n_a=0$, $j_a=0$) → HF ($n_b=2$, all j_b's) + H. Work will be resumed to theoretically verify the sideways scattering by considering such reactive transitions leading to the product molecule states of rotational angular momenta other than $j_b=0$.

Finally, we would like to note that the present study can be regarded as a case study since the DWBA quantitative results are subject to change depending on the choice of the potential surface. The Muckerman *V* LEPS potential surface we

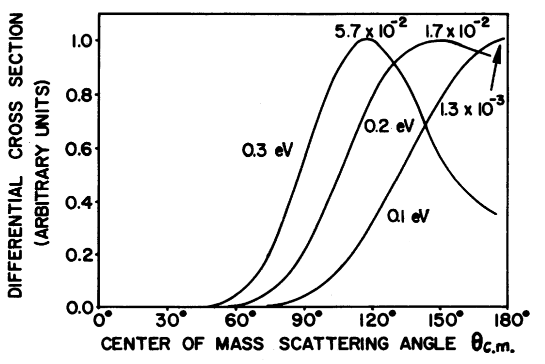

FIG. 3. Angular distributions for the state-to-state reactive transition of $F+H_2$ ($n_a=0$, $j_a=0$) → HF ($n_b=2$, $j_b=0$) at the incident kinetic energies of 0.1, 0.2, and 0.3 eV. The numbers are to indicate the peak values of the angular distributions at these incident kinetic energies.

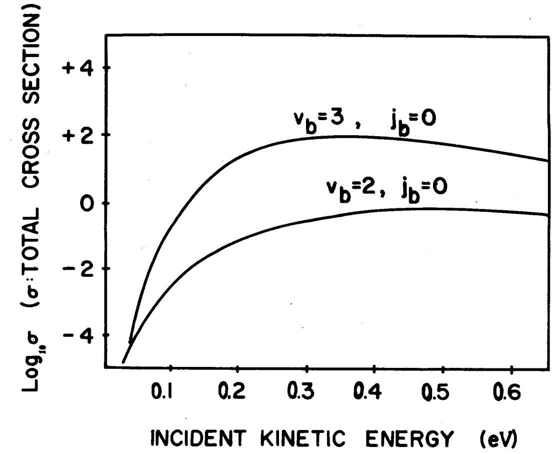

FIG. 4. Excitation functions for reactive transitions from the reactant molecule state of ($n_a=0$, $j_a=0$) to the product molecule states of ($n_b=2$, $j_b=0$) and ($n_b=3$, $j_b=0$), respectively.

have used in this study is not yet fully verified with experiments.

VI. CONCLUSION

A DWBA study made here is by no means exhaustive. Since one of our main objectives is to discuss physical factors that govern the angular distributions of scattered products, no comparative study has been made. For improvements, the present DWBA can be extended to include the coupling effects, by introducing coupled-channel wave functions in place of the elastic-scattering (distorted-) wave functions. The perturbation potential will be accordingly changed. Such CCBA[20] (coupled-channel Born-approximation) study is currently underway.

Other ways of improving the present DWBA treatment is the use of the diatomic-molecule wave functions which are coupled with the projectile motions. Such DWBA studies have been previously studied by others.[12] Their studies indicated marked differences in the magnitudes of the cross sections between the perturbed and unperturbed molecule treatments. On the other hand, it is to be noted that the other method known as Franck-Condon model[21] predicted notable differences in the widths of the angular distributions. The comparison of our DWBA method with the latter is less direct due to the differences in formalisms. We plan to examine the perturbed molecule case by using our own DWBA method for the sake of consistency.

In conclusion, we note from the DWBA study of direct reactive collision that the following hold true.

(1) Backward scattering in the product angular distribution is explainable from the examination of the kernel distribution for the atom–diatomic-molecule system in which the intermolecular interaction between the product molecule and projectile atom is repulsive.

(2) At high incident kinetic energies, sideways scattering is predicted to occur in the state-to-state reactive scattering.

(3) For identical triatomic systems, the magnitude of the cross section will be largest at the incident kinetic energy where wave-number matching occurs. However, unlike the case of a few nucleon transfer reaction involving a massive target nucleus, the conditions of wave-number matching for heterotriatomic systems is not always sufficient to yield the maximum cross section.

(4) The preferential transferred angular momentum is expected to be, often, other than 0 (even in the case of wave-number matching) unless $|K_a R_a - K_b R_b| = 0$.

(5) The kernel is seen to well define the reaction zone with the removal of the region interior to the channel radii where the classical turning points occur.

Despite the shortcomings of the present DWBA approach, it is expected that the conclusions made above will, in general, hold true.

ACKNOWLEDGMENT

One (S.H.S.) of the authors is grateful to Professor R. B. Bernstein and Professor R. D. Levine for their early encouragements and discussions. Professor R. E. Wyatt is also gratefully acknowledged for his discussions with the author (S.H.S.) on several occasions in the past. The authors are thankful to the University of Missouri-Rolla for the computational support.

---

[1] M. Gell-Mann and M. L. Goldberger, Phys. Rev. 91, 398 (1953).

[2] W. Tobocman, *Theory of Direct Nuclear Reactions* (Oxford University Press, London, 1961).

[3] R. G. Newton, *Scattering Theory of Waves and Particles* (McGraw-Hill, New York, 1966).

[4] M. L. Goldberger and K. M. Watson, *Collision Theory* (Wiley, New York, 1964).

[5] G. R. Satchler, Nucl. Phys. 55, 1 (1964).

[6] N. Austern, R. M. Drisco, E. C. Halbert, and G. R. Satchler, Phys. Rev. 133, B3 (1964).

[7] N. Austern, *Direct Nuclear Reaction Theories* (Wiley, New York, 1970).

[8] W. H. Miller, J. Chem. Phys. 49, 2373 (1968).

[9] R. D. Levine, Isr. J. Chem. 8, 13 (1970).

[10] K. T. Tang and M. Karplus, Phys. Rev. A 4, 1844 (1971).

[11] R. B. Walker and R. E. Wyatt, J. Chem. Phys. 61, 4839 (1974).

[12] K. T. Tang and B. H. Choi, J. Chem. Phys. 62, 3642 (1975); B. H. Choi and K. T. Tang, *ibid.* 63, 2854 (1975).

[13] S. H. Suck, Phys. Rev. A 15, 1893 (1977).

[14] S. H. Suck, Int. J. Quantum Chem. 16, 441 (1981).

[15] G. Racah, Phys. Rev. 62, 438 (1942).

[16] A. M. Arthurs and A. Dalgarno, Proc. Roy. Soc. London A256, 540 (1960).

[17] J. T. Muckerman, J. Chem. Phys. 56, 2997 (1972).

[18] Y. Shan, B. H. Choi, R. T. Poe, and K. T. Tang, Chem. Phys. Lett. 57, 379 (1978).

[19] R. K. Sparks, C. C. Hayden, K. Shobatake, D. M. Newmark, and Y. T. Lee, *Horizons of Quantum Chemistry* (Reidel, Boston, 1980), p. 91.

[20] T. Tamura, Phys. Rep. (section C of Phys. Lett.) 14, 59 (1974).

[21] C. L. Vila, D. J. Zvijac, and J. R. Ross, J. Chem. Phys. 70, 5362 (1979).